Continuous photocatalytic set-up assisted with nano TiO_2 plate for tannery wastewater treatment

Reza Shahbazi and Mona Zamani Pedram

ABSTRACT

A novel photocatalytic continuous system has been proposed for the treatment of tannery waste water, which has high levels of environmental pollutants. The purification process was performed by passing wastewater on a titanium dioxide (TiO_2)-coated surface, which is continuously activated by irradiation of ultraviolet light. To improve the yield of the process, ferric chloride ($FeCl_3$) was used as a coagulation agent. The organic and inorganic compounds, as well as the microorganisms in the tannery wastewater media, were degraded through a photocatalytic process. The results revealed that total dissolved solids and total suspended solids contents were significantly decreased from 8,450 and 8,990 mg·L^{-1} to 4,032 and 4,127 mg·L^{-1}, respectively. Furthermore, the chemical oxygen demand content of the sample was reduced from 370 to 50 mg·L^{-1} after the addition of 100 mL of $FeCl_3$ and 4 h of treatment. The same results were observed for the elimination of sulfate and chromium ions, which led to a decline in electrical conductivity. This suggests that introducing 100 mL of $FeCl_3$ as the coagulation agent and continuous treatment with photocatalityc set-up could be considered as an effective method for the purification of tannery wastewaters.

Key words | photocatalyst, photoreactor, tannery wastewater, TiO_2, wastewater

HIGHLIGHTS

- Continuous set-up fabricated for tannery wastewater treatment using photocatalytic reactions.
- TiO_2 photocatalyst activated by UV light for improvement of purification yield.
- $FeCl_3$, as coagulation agent, facilitated treatment by removing total dissolved solids.
- Toxic ions and microorganisms were eliminated in this method.

Reza Shahbazi
Mona Zamani Pedram (corresponding author)
Faculty of Mechanical Engineering-Energy Division,
K.N. Toosi University of Technology,
P.O. Box: 19395-1999, No. 15-19, Pardis St.,
Mollasadra Ave., Vanak Sq., Tehran 1999
143344,
Iran
E-mail: *m.zpedram@kntu.ac.ir*;
mona.zpedram@gmail.com

doi: 10.2166/wst.2021.164

GRAPHICAL ABSTRACT

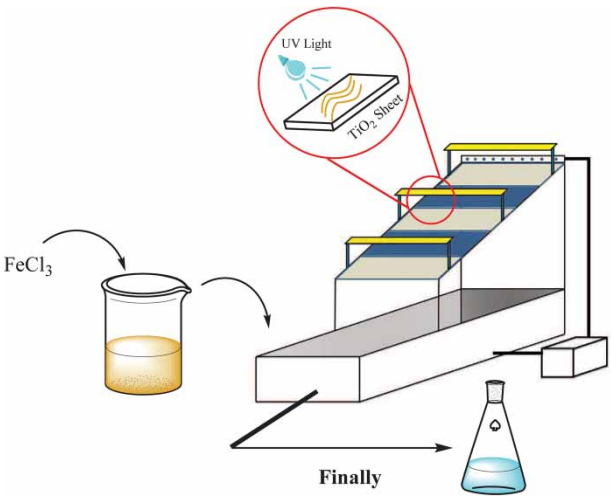

INTRODUCTION

Tanning is one of the oldest industries worldwide and began in ancient times by preparing leather for footwear, drums, and other musical instruments (Durai & Rajasimman 2011). Nowadays, leather tanning is a common industry particularly in Mediterranean countries, Middle East, and India (Insel *et al.* 2009; Mannucci *et al.* 2010; Natarajan *et al.* 2013). As the demand for leather has grown, the tanning industry developed from small places to the huge industrial districts. Moreover, the production process of the tanning progressed over the years and now consists of four main categories including: (1) hide and skin storage and beam house operations, (2) tanyard operations, (3) post-tanning operations, and (4) finishing operation (Lofrano *et al.* 2013). Despite the type of the production process this industry is considered as one the most hazardous industries due to high concentrations of pollutants with low biodegradability (Wang *et al.* 2019). The presence of the various cations and anions in tannery wastewater (TWW) leads to a high electrical conductivity and very low pH. In addition, the high concentration of solid components in the TWW in terms of total dissolved solids (TDS) and total suspended solids (TSS) restricts the implementation of many separation and purification methods. TWW also has high chemical oxygen demand (COD) and biological oxygen demand (BOD), which makes this pollutant wastewater unfavorable for different applications reuse (Al-Shaalan *et al.* 2019; Ali *et al.* 2019a, 2019b; Alothman *et al.* 2019; Khan *et al.* 2019). Furthermore, TWW could not be employed in agriculture due to the presence of hazardous ions, mainly Cr^{6+} and other toxic heavy metals. Numerous efforts have therefore been made to develop and improve the methods for TWW treatment and purification.

Using coagulation and flocculation agents is the most common method in purification of the TWWs. In this regards, aluminium sulfate ($AlSO_4$), ferric chloride ($FeCl_3$), and ferrous sulfate ($FeSO_4$) are the most common coagulation agents which effectively reduce COD, TSS, and toxic substances such as Cr^{6+}. Furthermore, biological treatment comprising aerobic and anaerobic processes, wetlands, and ponds is recognized as an efficient method for TWWs. It is worth mentioning that emerging treatment technologies have demonstrated significant advances in TWW purification (ALOthman 2012; Mittal *et al.* 2016; Ali *et al.* 2017, 2018; Alqadami *et al.* 2017, 2018; Alothman *et al.* 2020; Khan *et al.* 2020). Membrane processes, membrane bioreactors, adsorption, catalysis, and advanced oxidation process have received most attention during the last decade (Islam *et al.* 2018; Ahsan *et al.* 2019, 2020a, 2020b, 2020c, 2020d, 2021). Among these techniques, a number of studies have been carried out on the advanced oxidation processes. In this method, the production of highly reactive oxidizing agents, particularly active radical species, provides the opportunity of rapid and unselective oxidation for a broad range of organic compounds and biological species. Irradiation of UV light onto the TWW in addition to the presence of an appropriate photocatalyst to produce

reactive radicals has been investigated as effective method. The possible use of sunlight or near UV light is considered as a major advantage of this process, reducing the costs in large scale operations (Gogate & Pandit 2004). Although this method was not taken into account before 2007 (Schrank *et al.* 2004; Sauer *et al.* 2006), advances in nanotechnology has developed this method in the last decade. Degradation of TWW via dispersion of the green synthesized titanium dioxide (TiO_2) nanoparticles was carried out by Goutam *et al.* (2018). They reported that the 2.26% of COD and 76.48% of Cr^{6+} from TWW was removed by treatment with green synthesized TiO_2 nanoparticles, along with fabricated parabolic trough reactor. Bordes *et al.* reported that decoloration of TWW was successfully achieved by removing the organic components using plasma-sprayed TiO_2 coatings (Bordes *et al.* 2015). Evaluation of flower-like zinc oxide (ZnO) microspheres performance as a photocatalyst in the removal of Cr^{6+} in TWW was carried out by Liu *et al.* (2016). According to their report, Cr^{6+} ions were efficiently removed by ZnO hollow microspheres, which showed good photocatalytic stability. Moreover, critical parameters of BOD, COD, and TOC in TWW were reduced to 24%, 32%, and 30%, respectively, after only 180 min of exposure to the UV lamp. Removal of the chemical compounds was explored by Zhao *et al.* who proposed a novel synthetic method for TiO_2 nanoparticles (Zhao *et al.* 2017). They confirmed the applicability of the synthesized nanoparticles in TWW treatment by evaluating the organic component degradation kinetic. More recently, remarkable results have been achieved via treatment of TWW with synthesized N-doped carbon quantum dots functionalized SnS_2 by Wang *et al.* (2019).

A review of the literature showed that availability, low cost, and high efficiency of the TiO_2 nanoparticles makes it of particular interest (Zhao *et al.* 2017). However, the TiO_2 nanoparticles dispersion in the media in batch systems is highlighted as a major challenge at an industrial-scale. To overcome this, a continuous system has been designed in the current study using a TiO_2 nanoparticles-based photocatalyst coating embedded in novel experimental set-up. Moreover, TWW treatment performance has been improved through adding various amounts of $FeCl_3$ as a coagulation agent in the pre-treatment sequence to remove solid components in the sample, which is then followed by filtration (Figure 1). Next, the filtrate entered the advanced oxidation set-up to remove the other insoluble pollutants. The pH, electrical conductivity (EC), TDS, TSS, COD, and BOD were determined to evaluate the effectivity of the proposed treatment process on the quality of the purified TWW. The concentration of hazardous ionic components (chromium and sulfate ions) was also investigated.

EXPERIMENTAL

Materials and instruments

Nitric acid (HNO_3) (69%), $FeCl_3$ anhydrate (99%) NaOH (solid pellets, 98%) were purchased from Merck, Germany. TiO_2-P25 nanoparticles was supplied from Nanoshell, USA. The Fourier-transform infrared spectroscopy and attenuated total reflection infrared spectroscopy spectra were recorded using a Nicolete 800 instrument (Madison, USA) in the wavelength range of 400–4,000 cm^{-1}. The size and distribution of nanoparticles were investigated using a scanning electron microscope (SEM) MIRA-III TESCANE (Kohoutovice, Czech Republic). The TWW sample was collected from Misha Tannery Factory (Tehran, Iran) and the characteristic are shown in Table 1.

Fabrication of photocatalytic coating

The photocatalytic coating was fabricated by previously made titania powder (PMTP) thermal bonding method (Rao & Chaturvedi 2007). In this method, a suspension solution of TiO_2-P25 was prepared by adding nanoparticles (1 g) to 1 L of deionized water. Then, the pH of the suspension was adjusted to 3 by dropwise addition of HNO_3 solution (3 M) and the flask placed in an ultrasonic bath for 1 h at a frequency of 35 kHz. Preparation of the glass surface as the substrate for the TiO_2 coating was carried out by washing with hydrogen fluoride solution (5% v/v) and rinsing with sodium hydroxide (NaOH) solution (6 M) to remove any pollutants and increment of the hydroxyl groups on the glass surface, respectively. The obtained suspension was poured on the glass and placed in an oven at 80 °C for 16 h to thoroughly dry the surface. Then the plate was placed in a furnace for 3 h at 500 °C to establish the nanoparticles on the glass surface. Finally, the fabricated plates were washed with deionized water to remove any unsettled particle from their surfaces.

Preparation of the TWW sample

The TWW sample was obtained from Misha Tannery Factory and was pretreated. To remove the solid materials from the sample, the sample was filtered three times using Whatman filter paper with pore size of 0.45 µm. Then, the collected

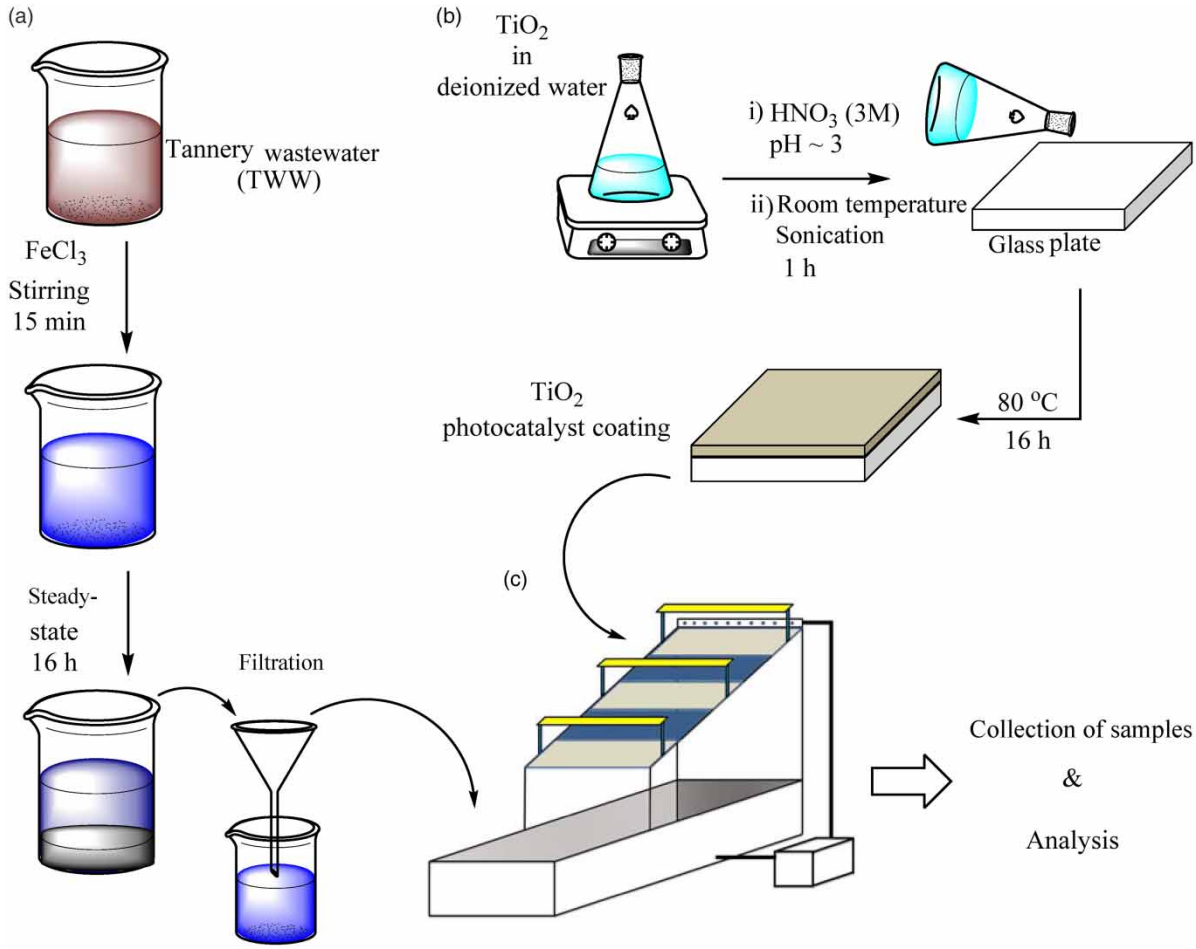

Figure 1 | The proposed method for the TWW treatment; (a) pretreatment of the sample with $FeCl_3$; (b) fabrication of the TiO_2 photocatalyst coating; (c) photocatalytic set-up.

Table 1 | The characteristics of the collected TWW

Parameter	Unit	Value
pH		3.99
Conductivity	$ms \cdot cm^{-1}$	10.24
Total solid	$mg \cdot L^{-1}$	8,990
TDS	$mg \cdot L^{-1}$	8,450
TSS	$mg \cdot L^{-1}$	540
COD	$mg \cdot L^{-1}$	370
BOD	$mg \cdot L^{-1}$	350
Sulfate	$mg \cdot L^{-1}$	1,180
Dichromium	$mg \cdot L^{-1}$	7.52

liquid phase was treated with $FeCl_3$ as the coagulation agent to precipitate the remaining suspended compounds in the media. The $FeCl_3$ was added in five different concentrations: 50, 100, 150, 200, and 250 mL per L of sample. Then, the samples were stirred at room temperature for 15 min to obtain a homogenous mixture, which changed the color of the suspension from turquoise blue to black. The stirring of samples was stopped for 24 h to allow the solids to form. Lastly, the liquid was filtered prior to final treatment in the set-up.

Fabrication of photoreactor and its performance

In the current study, the TWW treatment set-up was designed to provide a continuous flow system for the wastewater over the photocatalyst surface. For this, a set-up was made by cutting Plexiglas sheets using a computerized numerical control instrument. The cut sheets were joined to each other by an acrylic-based instant adhesive to form the plotted device as depicted in Figure 1. To run the device, the TWW was poured into the container after turning the UV lamps on. Then, the TWW flow was pumped

on the photocatalyst surface under UV irradiation of 365 nm from a 150 W UV light lamp. The TWW was agitated continuously by electrical agitators placed on the container floor during the treatment process (Figure 2).

Analysis methods

The pH of the samples were collected using a HANNA pH-meter. The EC was investigated by inoLab Cond 720 = . The COD and BOD of the treated TWW were evaluated using Standard Method 5220 D and Standard Method 5210 B, respectively. Standard Method 2540 C was used to estimate the total solid components, TDS, and TSS. The Cr^{6+} was determined using the Standard Method 3111 B Direct Air–Acetylene Flame Method. In this method, 100 mL of the sample was mixed with 1 mL 30% H_2O_2 before aspiration. The sulfate content was measured using the INSO – 2353 method.

RESULTS AND DISCUSSION

The structure of the prepared plates was investigated by FT-IR spectroscopy to confirm the sustainability of the TiO_2 nanoparticles after the preparation process steps. This test could be helpful to distinguish any change in the nano-TiO_2 structure during the hydrothermal process of attaching these particles on the glass sheet. Moreover, the FT-IR spectroscopy showed various functional groups in the TiO_2 nanoparticles, which were also determined by the transmission and absorptions range. According to the FT-IR results, the stretching vibration of the hydroxyl groups was observed around 3,500 cm^{-1} (Figure 3). There was also an absorbing band at 1,630 and 1,383 cm^{-1}, which could be assigned to the Ti–OH and related Ti–O bonds, respectively (León *et al.* 2017). Noteworthy, the most highlighted band at 690 cm^{-1} are considered as the characteristic peak of TiO_2 which is assigned to the Ti–O stretching vibration (Figure 3).

The surface of the prepared coatings was studied using SEM. The SEM images showed that the thickness of the TiO_2 coating on the glass surface was about 8.27 μm. Noteworthy, the size of the TiO_2 nanoparticles increased to about 56 nm due to agglomeration during the fabrication process – about 27 nm larger than the size of the particles before use (according to the supplier information) (Figure 4).

Evaluation of the total solid (TS) components including TDS and TSS was carried out using the Standard Method 2540 C/D method to explore the efficiency in removing

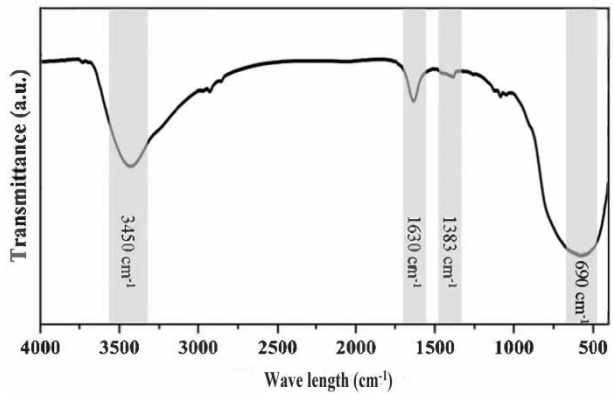

Figure 3 | FT-IR spectrum of TiO_2-coated plates.

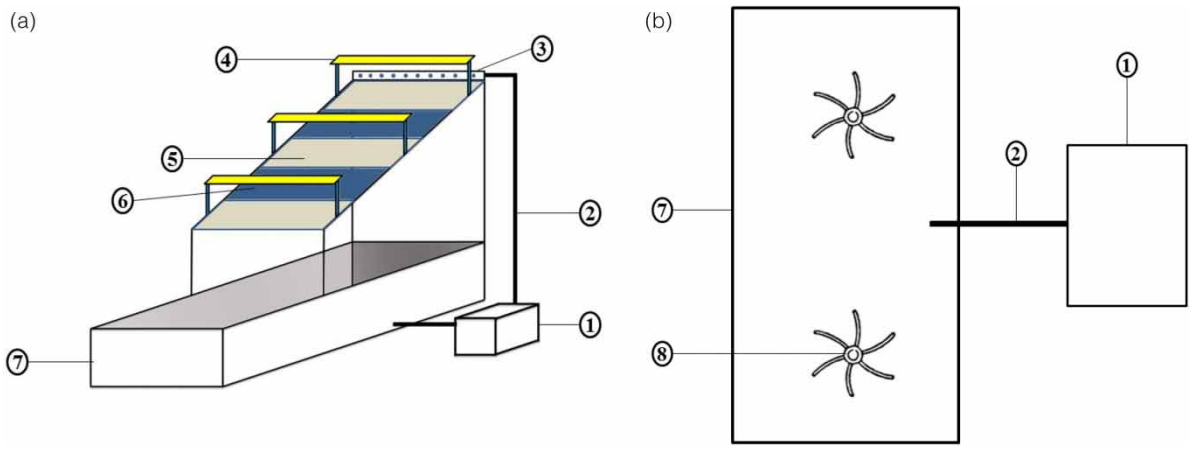

Figure 2 | Fabricated continuous water treatment device from front view (a) and bottom view (b) including the device parts: (1) pump; (2) pipe; (3) nozzles; (4) UV lamp; (5) TiO_2 photocatalyst coating; (6) Plexiglas sheets (7) container; and (8) curved agitator.

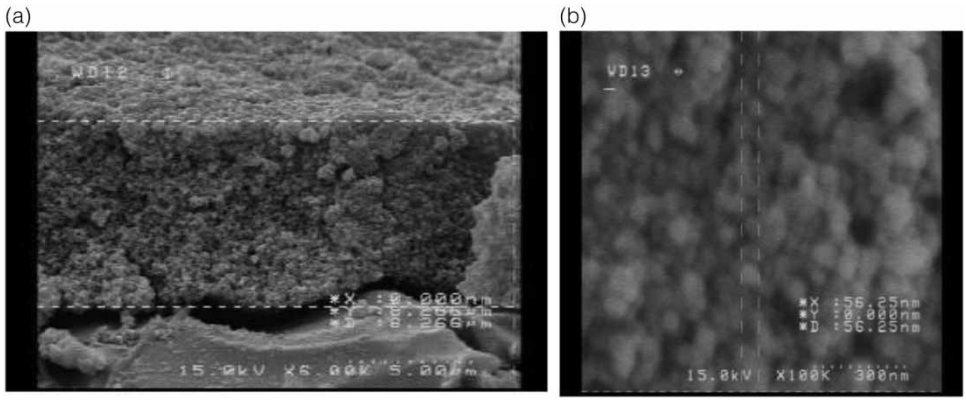

Figure 4 | The SEM images of the TiO_2 photocatalyst coatings.

the TDS and TSS from the TWW. The results revealed that the blank sample contained 8,990 mL·L^{-1} of TS including 8,450 and 540 mL·L^{-1} of TDS and TSS, respectively. These values were reduced to 5,437 and 134 mL·L^{-1} by adding 50 mL of $FeCl_3$ to the sample. The largest reduction was observed by adding 100 mL of $FeCl_3$, which led to TDS and TSS reducing to 4,032 and 95 mL·L^{-1} (Figure 5). Noteworthy, the addition of the higher content of $FeCl_3$ led to a slight increase in TS values compared to the concentration from adding 100 mL of $FeCl_3$. This result was achieved after introducing extra contents of coagulation agent into the samples which led to the formation of Fe-based complexes in the aqueous media. Consequently, the TDS and TSS values increased slightly after the addition of more than 150 mL of $FeCl_3$ and increased to 4,928 and 178.92 mL·L^{-1} in the sample containing 250 mL $FeCl_3$, respectively (Figure 5).

The treatment of the TWW was analyzed to evaluate the impact of each parameter on the quality of the purified water. Since pH, COD, BOD, and DO could be assumed to be the most important parameters in the purified wastewater, these parameters were evaluated for each sample. After the addition of the specified content of $FeCl_3$ as the coagulation agent, the samples were introduced into the photoreactor set-up and were collected at different times. According to the results, the addition of 50 mL of $FeCl_3$ into the TWW led to a decrease in pH to 1.30 (Figure 6). It was observed that the pH value of this sample increased from 4.81 to 5.28 by treating the TWW with the fabricated device and increasing the contact time. This trend was observed in other samples and it was confirmed that the pH value increased by prolonging the contact time (Figure 6). The changes in pH values were due to the presence of the calcium bicarbonate ($Ca(HCO_3)_2$) in the TWW

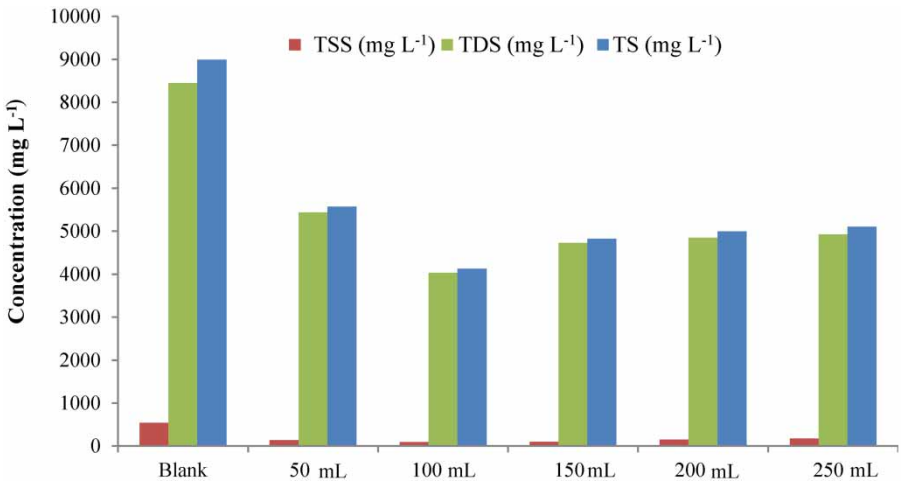

Figure 5 | The concentration of the solid components in the TWW samples.

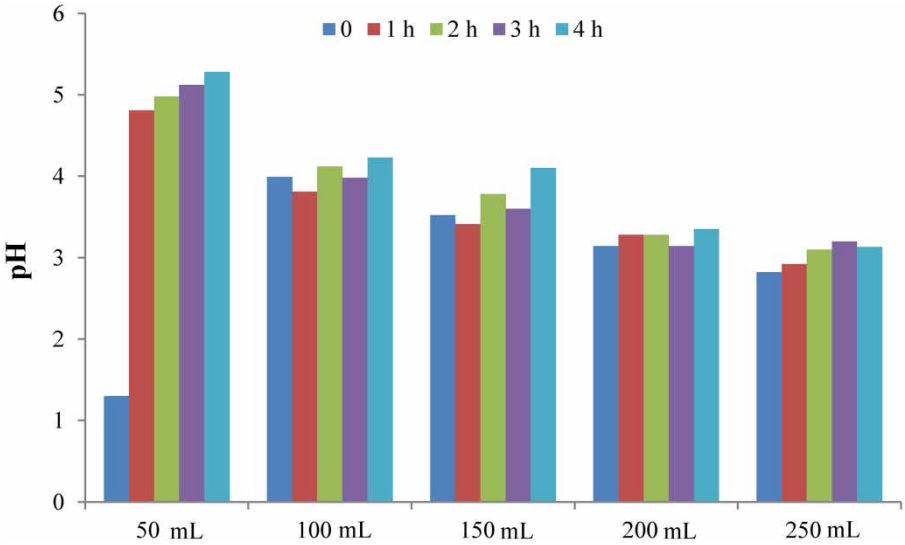

Figure 6 | The pH values of treated TWW samples from different contents of $FeCl_3$.

and its reaction with $FeCl_3$. In fact, the reaction between these two compounds leads to the formation of iron(II) hydroxide ($Fe(OH)_2$) and calcium chloride ($CaCl_2$) compounds. The basic nature of these two compounds was the reason for the pH increment in the treated TWW:

$$2FeCl_3 + 3Ca(HCO_3)_2 \rightarrow 2Fe(OH)_2 + 3CaCl_2 + 6CO_2 \quad (1)$$

On the other hand, conditions during the treatment process (long treatment time, UV light, low pH, and etc.) made it possible to form neutralized compounds from ionic species. Therefore, the EC changes were expected in the treated TWW samples. Investigation of the samples after termination of the treatment showed that the EC value was lower in all samples compared to the blank. Addition of 50 mL of coagulation agent into the TWW led to a reduction in the EC from 10.24 to 7.34 ms·cm^{-1} (Figure 7). This trend reached the minimum point in the sample containing 100 mL of $FeCl_3$ of about 4.62 ms·cm^{-1} (Figure 7). It should be noted that a further decrease in EC was not observed by introducing more $FeCl_3$ into the samples; contrarily a slight increase was observed in the EC value. The

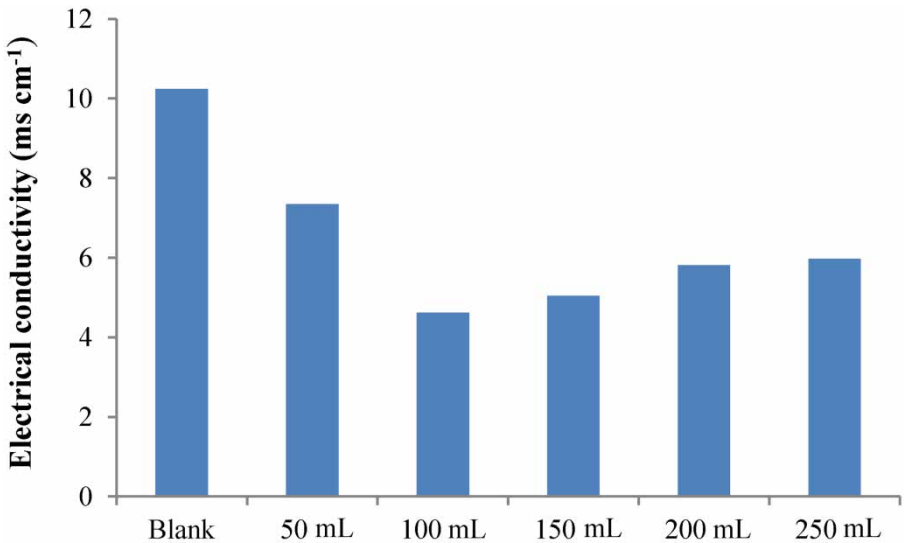

Figure 7 | The EC contents of the treated TWW samples.

observed increase could be related to the production of the Fe^{3+} and Cl^{-} ions in the aqueous media in relation to the excess content of the coagulation agent in the samples.

Evaluation of the COD parameter in the treated TWW could be considered as one of the most important analyses due to the presence of organic chemical compounds with high toxicity in TWW, such as phenolic compounds. The evaluation of the COD was performed using the Standard Method 5220 D in the current study. According to the results, the proposed method could effectively be used in degrading chemical compounds in the TWW samples (Figure 8). The COD content of the sample after the addition of 50 mL of the $FeCl_3$ into the TWW was about 370 mg·L^{-1}, which reduced to 50 mg·L^{-1} by passing the sample through the photocatalyst set-up for 4 h. Similarly, this trend was observed for other samples containing different contents of $FeCl_3$. In particular, the addition of the 100, 150, and 200 mL of coagulation agent led to the reduction of the chemical components in the TWW after 4 h treatment with TiO_2 coating and UV light radiation. Accordingly, it could be assumed that the fabricated set-up was able to active radical hydroxyl groups on the surface of the photocatalyst coating. In this mechanism, electrons (e^{-}) were induced from valance band (VB) to conduction band (CB) by absorbing a photon with upper energy rather than the band gap energy. This phenomenon led to the formation of an electron vacancy in the VB which is called a hole (h^{+}) (Equation (2)). Afterwards, various radical compounds might be formed through different reactions to degrade the chemical compounds. Determining all the produced radical intermediates in the TWW was impossible due to the presence of a wide range of organic and inorganic compounds in the aqueous media which produced intermediate radicals. Rare radicals and products in photocatalyst degradation of the TWW are known (Natarajan *et al.* 2013). Therefore, only produced radicals in the TWW treatment were considered in the current study. The radical hydroxyl group, which is known as one of the most active compounds in the degradation of chemical components was produced via the reaction between the hole in the VB (h^{+}_{VB}) and water in the TWW (Equation (3)). Furthermore, the other radically active compounds were produced in simultaneous reactions that were responsible for the observed high COD degradation efficiency.

$$TiO_2 + h\nu \rightarrow e^{-}_{CB} + h^{+}_{VB} \quad (2)$$

$$h^{+}_{VB} + H_2O \rightarrow TiO_2 + H^{+} + OH^{\bullet} \quad (3)$$

$$e^{-}_{CB} + O_2 \rightarrow TiO_2 + O_2^{\bullet -} \quad (4)$$

$$O_2^{\bullet -} + H^{+} \rightarrow HO_2^{\bullet} \quad (5)$$

$$2O_2^{\bullet -} + 2H^{+} \rightarrow O_2 + H_2O_2 \quad (6)$$

$$H_2O_2 + e^{-}_{CB} \rightarrow OH^{\bullet} + OH^{-} \quad (7)$$

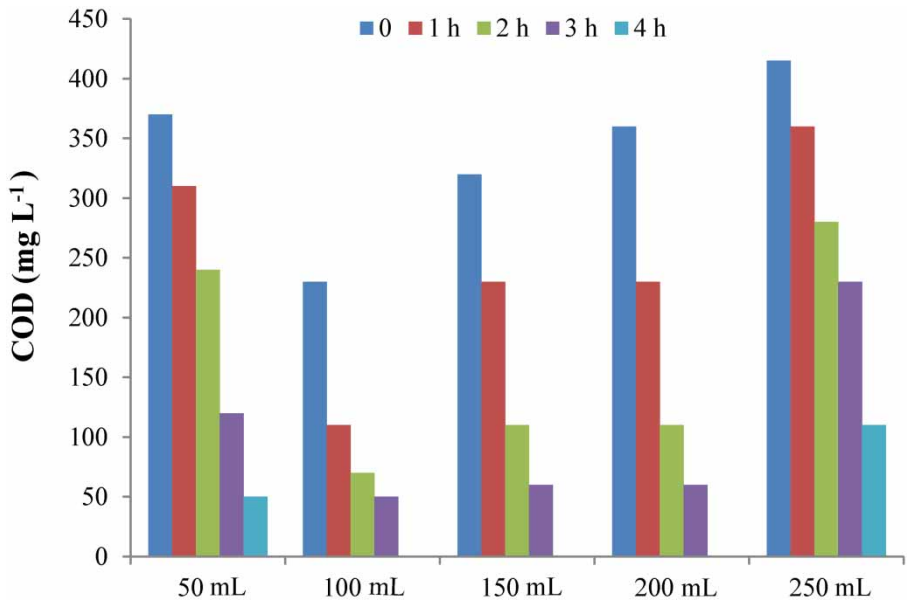

Figure 8 | Comparison between COD values of treated TWW samples.

Considering that the biological species could be degraded by radical components, it was assumed that treating the TWW with the novel designed set-up could reduce the BOD content of the sample. This assumption was confirmed by evaluation of the BOD using the Standard Method 5210 B. Accordingly, the BOD content was reduced during the time it was in contact with the photocatalyst surface under UV light (Figure 9). It was observed that the BOD content reached to zero after 4 h in all samples except for the sample containing 50 mL of $FeCl_3$, which is probably because of the low concentration of the coagulation agent. Nevertheless, the reducing trend of the BOD concentration in all samples revealed that the proposed method could be highlighted as an effective method in the degradation of both chemically and biologically toxic species.

Since sulfuric acid and sulfide are two essentials for leather tannery, removing the sulfate (SO_4^{2-}) is important in the purification of the TWW. Noteworthy is that sulfide in the unhairing process oxidizes to sulfate, and therefore, the sulfate group is the only sulfur-based contaminant in TWW. It could be assumed that the $FeSO_4$ could be formed in the TWW samples due to the insertion of $FeCl_3$ as a coagulation agent in the first steps of the treatment process. Therefore, sulfate concentration was evaluated after the process finished. The results revealed that the sulfate content decreased from 1,180 $mg{\cdot}L^{-1}$ in the blank sample to 900 $mg{\cdot}L^{-1}$ by adding 50 mL of $FeCl_3$ to the sample (Figure 10(a)). Increasing the coagulation agent content to 100 mL caused a further reduction in sulfate content of the sample to 700 $mg{\cdot}L^{-1}$. However, adding more $FeCl_3$ led to sulfate concentrations greater than 700 $mg{\cdot}L^{-1}$ (Figure 10(a)). Because the coagulation of the SO_4^{2-} depended on the saturation Cl^-, the separation of the SO_4^{2-} decreased when the solution was saturated by Cl^-. Therefore, the removal of SO_4^{2-} in concentrations above 700 $mg{\cdot}L^{-1}$ was reduced. Furthermore, the removal of Cr^{6+} in the TWW is highlighted as one the most important steps in the purification processes. Therefore, monitoring the Cr^{6+} ion elimination in the form of dichromate ($Cr_2O_7^{2-}$) was one of the main goals in the current study using the atomic absorption Standard Method 3111 B. The concentration of $Cr_2O_7^{2-}$ in the blank sample was 7.52 $mg{\cdot}L^{-1}$, which was about four times greater than the standard value (Figure 8(b)). This was reduced to 3.78 and 0.37 $mg{\cdot}L^{-1}$ by adding 50 mL and 100 mL of $FeCl_3$, respectively, and passing through the photoreactor for 4 h. Comparison between the reported related literatures and the final concentration in the sample containing 100 mL of $FeCl_3$ revealed that the proposed process could be considered as a method in TWW purification. In fact, the concentration was close to the minimum standard content of the Cr^{6+} in the purified TWW. The probable mechanism for degradation of $Cr_2O_7^{2-}$ was the production of the electron and H_3O^+ ion in Equations (2) and (3). These two species could react with $Cr_2O_7^{2-}$ to produce the chrome(III) ion (Cr^{3+}) (Equation (8)). Noticeably, increasing the $FeCl_3$ content to 150, 200, and 250 mL in the TWW samples led to an increase of the $Cr_2O_7^{2-}$ concentration in the sample (Figure 8(b)). This result could be explained by the presence of the free Cl^- ions obtained

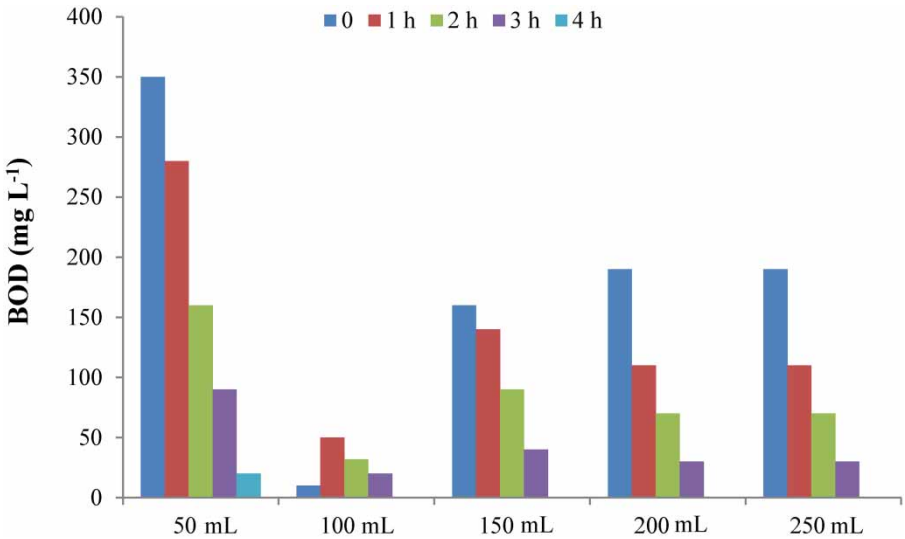

Figure 9 | The BOD values of the treated TWW samples.

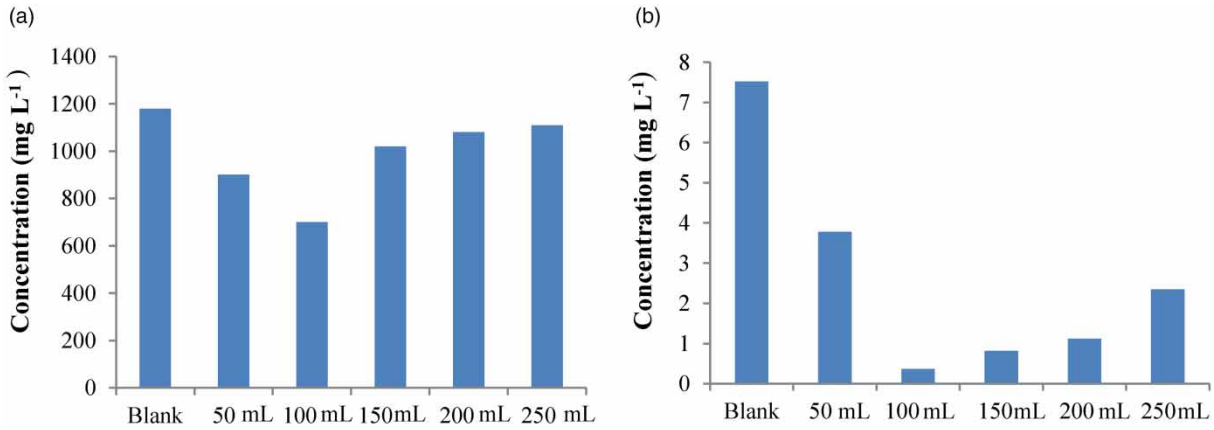

Figure 10 | The concentration of sulfate (a) and chromium (b) ions in different samples.

from the excess amount of $FeCl_3$ in the media which was surrounded by H^+ ions. This phenomenon might affect the $Cr_2O_7^{2-}$ removal reaction because of the reduction of the H^+ concentration in the treated sample.

$$Cr_2O_7^{2-} + 14\,H^+ + 6\,e^- \rightarrow 2Cr^{3+} + 7H_2O \quad (8)$$

According to the observed results in the analysis of the TWW samples, introducing 100 mL of $FeCl_3$ could be considered as the optimum content for coagulation agent. In this content, all contaminant parameters could be reduced to standard values or be close to the acceptable range for treated TWW. All the tests and experiments were repeated three times in the same manner using 100 mL of $FeCl_3$ to confirm the process reliability and accuracy. The results showed that the proposed process could be presented as a novel method with high accuracy.

CONCLUSION

Continuous set-up for treatment of the TWW has been fabricated using TiO_2 nanoparticles as photocatalyst agent. To overcome the disadvantages of the dispersed nanoparticles, the photocatalyst was established on the glass sheets using the PMTP method, including thermal conjugation of the TiO_2 nanoparticles on the glass sheets. The TWW was first treated with $FeCl_3$ as coagulation agent to improve the elimination yield of the pollutants. This step was followed by passing the wastewater sample on the photocatalyst sheet under UV light for various time durations. The results revealed that all the effective water quality parameters improved in the TWW sample. Evaluation of the sample pH revealed that it increased to 4–5 at the end of the process. Moreover, the EC of the samples decreased by removing the ions in purification steps from 10.24 to 4.62 $ms{\cdot}cm^{-1}$. Noteworthy is that the coagulation agent had an important role on the removal of the solid components. Specifically, introducing 100 mL of $FeCl_3$ into the wastewater led to a reduction in the total solid content to 4,127 $mg{\cdot}L^{-1}$. Degradation of the oxygen was confirmed by COD and BOD test. According to these tests COD compounds were completely removed and the BOD content was reduced to 20 $mg{\cdot}L^{-1}$. Furthermore, the concentration of the SO_4^{2-} and $Cr_2O_7^{2-}$ decreased to 700 and 0.37 $mg{\cdot}L^{-1}$, which was in the standard range for treated TWW. Conclusively, introducing 100 mL of $FeCl_3$ as a coagulation agent and continuous treatment in the photoreactor for 4 h was found to be the optimal procedure for treating TWW. The accuracy and reliability of the proposed procedure was confirmed by repeating the experimental tests three times.

DATA AVAILABILITY STATEMENT

All relevant data are included in the paper or its Supplementary Information.

REFERENCES

Ahsan, M. A., Deemer, E., Fernandez-Delgado, O., Wang, H., Curry, M. L., El-Gendy, A. A. & Noveron, J. C. 2019 Fe nanoparticles encapsulated in MOF-derived carbon for the reduction of 4-nitrophenol and methyl orange in water. *Catalysis Communications* **130**, 105753.

Ahsan, M. A., Imam, M. A., Santiago, A. R. P., Rodriguez, A., Alvarado-Tenorio, B., Bernal, R., Luque, R. & Noveron, J. C.

2020a Spent tea leaves templated synthesis of highly active and durable cobalt-based trifunctional versatile electrocatalysts for hydrogen and oxygen evolution and oxygen reduction reactions. *Green Chemistry* **22** (20), 6967–6980.

Ahsan, M. A., Puente Santiago, A. R., Hong, Y., Zhang, N., Cano, M., Rodriguez-Castellon, E., Echegoyen, L., Sreenivasan, S. T. & Noveron, J. C. 2020b Tuning of trifunctional NiCu bimetallic nanoparticles confined in a porous carbon network with surface composition and local structural distortions for the electrocatalytic oxygen reduction, oxygen and hydrogen evolution reactions. *Journal of the American Chemical Society* **142** (34), 14688–14701.

Ahsan, M. A., Santiago, A. R. P., Nair, A. N., Weller, J. M., Sanad, M. F., Valles-Rosales, D. J., Chan, C. K., Sreenivasan, S. & Noveron, J. C. 2020c Metal-organic frameworks-derived multifunctional carbon encapsulated metallic nanocatalysts for catalytic peroxymonosulfate activation and electrochemical hydrogen generation. *Molecular Catalysis* **498**, 111241.

Ahsan, M. A., Santiago, A. R. P., Rodriguez, A., Maturano-Rojas, V., Alvarado-Tenorio, B., Bernal, R. & Noveron, J. C. 2020d Biomass-derived ultrathin carbon-shell coated iron nanoparticles as high-performance tri-functional HER, ORR and Fenton-like catalysts. *Journal of Cleaner Production* **275**, 124141.

Ahsan, M. A., Santiago, A. R. P., Sanad, M. F., Weller, J. M., Fernandez-Delgado, O., Barrera, L. A., Maturano-Rojas, V., Alvarado-Tenorio, B., Chan, C. K. & Noveron, J. C. 2021 Tissue paper-derived porous carbon encapsulated transition metal nanoparticles as advanced non-precious catalysts: carbon-shell influence on the electrocatalytic behaviour. *Journal of Colloid and Interface Science* **581**, 905–918.

Ali, I., Alothman, Z. A. & Alwarthan, A. 2017 Supra molecular mechanism of the removal of 17-β-estradiol endocrine disturbing pollutant from water on functionalized iron nano particles. *Journal of Molecular Liquids* **241**, 123–129.

Ali, I., Alharbi, O. M. L., Alothman, Z. A. & Badjah, A. Y. 2018 Kinetics, thermodynamics, and modeling of amido black dye photodegradation in water using Co/TiO_2 nanoparticles. *Photochemistry and Photobiology* **94** (5), 935–941.

Ali, I., Alharbi, O. M. L., Alothman, Z. A., Al-Mohaimeed, A. M. & Alwarthan, A. 2019a Modeling of fenuron pesticide adsorption on CNTs for mechanistic insight and removal in water. *Environmental Research* **170**, 389–397.

Ali, I., Alharbi, O. M. L., Alothman, Z. A., Alwarthan, A. & Al-Mohaimeed, A. M. 2019b Preparation of a carboxymethylcellulose-iron composite for uptake of atorvastatin in water. *International Journal of Biological Macromolecules* **132**, 244–253.

ALOthman, Z. A. 2012 A review: fundamental aspects of silicate mesoporous materials. *Materials* **5** (12), 2874–2902.

Alothman, Z. A., Badjah, A. Y. & Ali, I. 2019 Facile synthesis and characterization of multi walled carbon nanotubes for fast and effective removal of 4-tert-octylphenol endocrine disruptor in water. *Journal of Molecular Liquids* **275**, 41–48.

Alothman, Z. A., Bahkali, A. H., Khiyami, M. A., Alfadul, S. M., Wabaidur, S. M., Alam, M. & Alfarhan, B. Z. 2020 Low cost biosorbents from fungi for heavy metals removal from wastewater. *Separation Science and Technology* **55** (10), 1766–1775.

Alqadami, A. A., Naushad, M., Abdalla, M. A., Ahamad, T., Abdullah Alothman, Z., Alshehri, S. M. & Ghfar, A. A. 2017 Efficient removal of toxic metal ions from wastewater using a recyclable nanocomposite: a study of adsorption parameters and interaction mechanism. *Journal of Cleaner Production* **156**, 426–436.

Alqadami, A. A., Khan, M. A., Siddiqui, M. R. & Alothman, Z. A. 2018 Development of citric anhydride anchored mesoporous MOF through post synthesis modification to sequester potentially toxic lead (II) from water. *Microporous and Mesoporous Materials* **261**, 198–206.

Al-Shaalan, N. H., Ali, I., Alothman, Z. A., Al-Wahaibi, L. H. & Alabdulmonem, H. 2019 High performance removal and simulation studies of diuron pesticide in water on MWCNTs. *Journal of Molecular Liquids* **289**, 111039.

Bordes, M. C., Vicent, M., Moreno, R., García-Montaño, J., Serra, A. & Sánchez, E. 2015 Application of plasma-sprayed TiO_2 coatings for industrial (tannery) wastewater treatment. *Ceramics International* **41** (10, Part B), 14468–14474.

Durai, G. & Rajasimman, M. 2011 Biological treatment of tannery wastewater: a review. *Journal of Environmental Science and Technology* **4** (1), 1–17.

Gogate, P. R. & Pandit, A. B. 2004 A review of imperative technologies for wastewater treatment I: oxidation technologies at ambient conditions. *Advances in Environmental Research* **8** (3–4), 501–551.

Goutam, S. P., Saxena, G., Singh, V., Yadav, A. K., Bharagava, R. N. & Thapa, K. B. 2018 Green synthesis of TiO_2 nanoparticles using leaf extract of *Jatropha curcas* L. for photocatalytic degradation of tannery wastewater. *Chemical Engineering Journal* **336**, 386–396.

Insel, H. G., Görgün, E., Artan, N. & Orhon, D. 2009 Model based optimization of nitrogen removal in a full scale activated sludge plant. *Environmental Engineering Science* **26** (3), 471–480.

Islam, M. T., Saenz-Arana, R., Hernandez, C., Guinto, T., Ahsan, M. A., Kim, H., Lin, Y., Alvarado-Tenorio, B. & Noveron, J. C. 2018 Adsorption of methylene blue and tetracycline onto biomass-based material prepared by sulfuric acid reflux. *RSC Advances* **8** (57), 32545–32557.

Khan, M. A., Alqadami, A. A., Otero, M., Siddiqui, M. R., Alothman, Z. A., Alsohaimi, I., Rafatullah, M. & Hamedelniel, A. E. 2019 Heteroatom-doped magnetic hydrochar to remove post-transition and transition metals from water: synthesis, characterization, and adsorption studies. *Chemosphere* **218**, 1089–1099.

Khan, M. A., Alqadami, A. A., Wabaidur, S. M., Siddiqui, M. R., Jeon, B.-H., Alshareef, S. A., Alothman, Z. A. & Hamedelniel, A. E. 2020 Oil industry waste based non-magnetic and magnetic hydrochar to sequester potentially toxic post-transition metal ions from water. *Journal of Hazardous Materials* **400**, 123247.

León, A., Reuquen, P., Garín, C., Segura, R., Vargas, P., Zapata, P. & Orihuela, P. A. 2017 FTIR and Raman characterization of TiO_2 nanoparticles coated with polyethylene glycol as carrier for 2-methoxyestradiol. *Applied Sciences* **7** (1), 49.

Liu, J., Zhao, Y., Ma, J., Dai, Y., Li, J. & Zhang, J. 2016 Flower-like ZnO hollow microspheres on ceramic mesh substrate for photocatalytic reduction of Cr(VI) in tannery wastewater. *Ceramics International* **42** (14), 15968–15974.

Lofrano, G., Meriç, S., Zengin, G. E. & Orhon, D. 2013 Chemical and biological treatment technologies for leather tannery chemicals and wastewaters: a review. *Science of the Total Environment* **461–462**, 265–281.

Mannucci, A., Munz, G., Mori, G. & Lubello, C. 2010 Anaerobic treatment of vegetable tannery wastewaters: a review. *Desalination* **264** (1), 1–8.

Mittal, A., Naushad, M., Sharma, G., Alothman, Z. A., Wabaidur, S. M. & Alam, M. 2016 Fabrication of MWCNTs/tho2 nanocomposite and its adsorption behavior for the removal of Pb(II) metal from aqueous medium. *Desalination and Water Treatment* **57** (46), 21863–9.

Natarajan, T. S., Natarajan, K., Bajaj, H. C. & Tayade, R. J. 2013 Study on identification of leather industry wastewater constituents and its photocatalytic treatment. *International Journal of Environmental Science and Technology* **10** (4), 855–864.

Rao, N. N. & Chaturvedi, V. 2007 Photoactivity of TiO_2-coated pebbles. *Industrial & Engineering Chemistry Research* **46** (13), 4406–4414.

Sauer, T. P., Casaril, L., Oberziner, A. L. B., José, H. J. & Moreira, R. d. F. P. M. 2006 Advanced oxidation processes applied to tannery wastewater containing Direct Black 38–Elimination and degradation kinetics. *Journal of Hazardous Materials* **135** (1–3), 274–279.

Schrank, S. G., José, H. J., Moreira, R. F. P. M. & Schröder, H. F. 2004 Elucidation of the behavior of tannery wastewater under advanced oxidation conditions. *Chemosphere* **56** (5), 411–423.

Wang, S., Li, L., Zhu, Z., Zhao, M., Zhang, L., Zhang, N., Wu, Q., Wang, X. & Li, G. 2019 Remarkable improvement in photocatalytic performance for tannery wastewater processing via sns2 modified with N-doped carbon quantum dots: synthesis, characterization, and 4-Nitrophenol-Aided Cr(VI) photoreduction. *Small* **15** (29), 1804515.

Zhao, W., He, X., Peng, Y., Zhang, H., Sun, D. & Wang, X. 2017 Preparation of mesoporous TiO_2 with enhanced photocatalytic activity towards tannery wastewater degradation. *Water Science and Technology* **75** (6), 1494–1499.

First received 17 February 2021; accepted in revised form 13 April 2021. Available online 28 April 2021